



MENU ▾

803.EMERGING DIAGNOSTIC TOOLS AND TECHNIQUES | NOVEMBER 5, 2020

## A Deep Learning Framework for Sickle Cell Disease Microfluidic Biomarker Assays

Niksa Praljak, Brandon Shipley, Ayesha Gonzales, Utku Goreke, MSc, Shamreen Iram, Gundeep Singh, Ailis Hill, Umut A. Gurkan, PhD, Michael Hinczewski, PhD



*Blood* (2020) 136 (Supplement 1): 15–16.

<https://doi.org/10.1182/blood-2020-141693>

Split-Screen



Share ▾



Tools ▾

**Introduction:** Vaso-occlusive crises (VOCs) are a leading cause of morbidity and early mortality in individuals with sickle cell disease (SCD). These crises are triggered by sickle red blood cell (sRBC) aggregation in blood vessels and are influenced by factors such as enhanced sRBC and white blood cell (WBC) adhesion to inflamed endothelium. Advances in microfluidic biomarker assays (i.e., SCD Biochip systems) have led to clinical studies of blood cell adhesion onto endothelial proteins, including, fibronectin, laminin, P-selectin, ICAM-1, functionalized in microchannels. These microfluidic assays allow mimicking the physiological aspects of human microvasculature and help characterize biomechanical properties of adhered sRBCs under flow. However, analysis of the microfluidic biomarker assay data has so far relied on manual cell counting and exhaustive visual morphological characterization of cells by trained personnel. Integrating deep learning algorithms with microscopic imaging of adhesion protein functionalized microfluidic channels can accelerate and standardize accurate classification of blood cells in microfluidic biomarker assays. Here we present a deep learning approach into a general-purpose analytical tool covering a wide range of conditions: channels functionalized with different proteins (laminin or P-selectin), with varying degrees of adhesion by both sRBCs and WBCs, and in both normoxic and hypoxic environments.

**Methods:** Our neural networks were trained on a repository of manually labeled SCD Biochip microfluidic biomarker assay whole channel images. Each channel contained adhered cells pertaining to clinical whole sblood under constant shear stress of 0.1 Pa, mimicking physiological levels in post-capillary venules. The machine learning (ML) framework consists of two phases: Phase I segments pixels belonging to blood cells adhered to the microfluidic channel surface, while Phase II associates pixel clusters with specific cell types

(sRBCs or WBCs). Phase I is implemented through an ensemble of seven generative fully convolutional neural networks, and Phase II is an ensemble of five neural networks based on a Resnet50 backbone. Each pixel cluster is given a probability of belonging to one of three classes: adhered sRBC, adhered WBC, or non-adhered / other.

**Results and Discussion:** We applied our trained ML framework to 107 novel whole channel images not used during training and compared the results against counts from human experts. As seen in **Fig. 1A**, there was excellent agreement in counts across all protein and cell types investigated: sRBCs adhered to laminin, sRBCs adhered to P-selectin, and WBCs adhered to P-selectin. Not only was the approach able to handle surfaces functionalized with different proteins, but it also performed well for high cell density images (up to 5000 cells per image) in both normoxic and hypoxic conditions (**Fig. 1B**). The average uncertainty for the ML counts, obtained from accuracy metrics on the test dataset, was 3%. This uncertainty is a significant improvement on the 20% average uncertainty of the human counts, estimated from the variance in repeated manual analyses of the images. Moreover, manual classification of each image may take up to 2 hours, versus about 6 minutes per image for the ML analysis. Thus, ML provides greater consistency in the classification at a fraction of the processing time. To assess which features the network used to distinguish adhered cells, we generated class activation maps (**Fig. 1C-E**). These heat maps indicate the regions of focus for the algorithm in making each classification decision. Intriguingly, the highlighted features were similar to those used by human experts: the dimple in partially sickled RBCs, the sharp endpoints for highly sickled RBCs, and the uniform curvature of the WBCs. Overall the robust performance of the ML approach in our study sets the stage for generalizing it to other endothelial proteins and experimental conditions, a first step toward a universal microfluidic ML framework targeting blood disorders. Such a framework would not only be able to integrate advanced biophysical characterization into fast, point-of-care diagnostic devices, but also provide a standardized and reliable way of monitoring patients undergoing targeted therapies and curative interventions, including, stem cell and gene-based therapies for SCD.

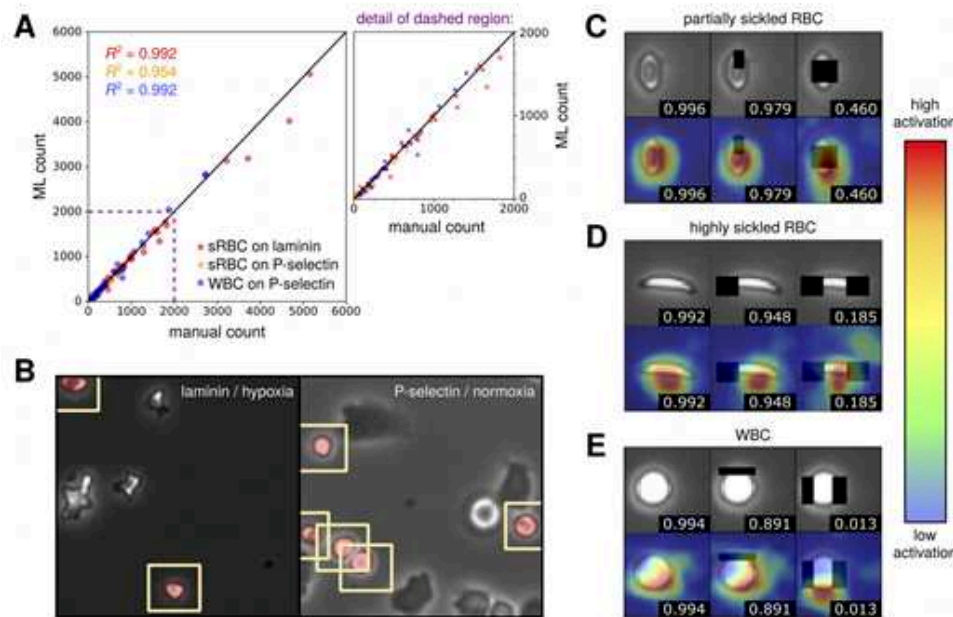


**Figure 1. A deep learning framework for sickle cell disease microfluidic biomarker assays.** (A) Comparison of machine learning (ML) versus manual counts by human experts for 107 images of microfluidic channels. The channels were functionalized with either P-selectin or laminin: the blue and orange points respectively correspond to counts of sRBCs and WBCs adhered to P-selectin, while the red points correspond to sRBCs adhered to laminin. (B) Two examples of input image tiles for the ML algorithm, overlaid with the predicted segmentation masks generated by Phase I of the network (identifying pixels belonging to either adhered sRBC or WBC in red). The left tile is for a laminin-functionalized channel under hypoxic conditions, while the right is for a P-selectin functionalized channel under normoxic conditions. The network is able to identify adhered cells despite the presence of cellular debris, out-of-focus cells (not adhered to the functionalized proteins), and variations in background brightness. Computed bounding boxes, used to crop the cells for input into Phase II, are shown in yellow. (C-E) Class activation maps for representative cell types, highlighting the cell features that allow the Phase II network to classify each cell as either an sRBC or WBC. Top rows show the original images, while bottom rows show activation heat maps. The regions with highest activation (shaded red) are those that are most important for network to make its decision. The left column shows the original image, while the center and right columns are images intentionally modified to remove certain regions (black blocks) in order to confuse the network. The number in each panel is the probability assigned by the network of the cell being an sRBC (C, D) or a WBC (E). For the partially sickled RBC in (C) the network still classifies accurately when part of the dimple is blocked, but the certainty drops when the entire dimple is blocked. Hence for these types of cells the dimple is the key distinguishing feature. Analogously for the highly sickled RBC cell in (D) the network needs to see at least one sharp endpoint to classify reliably, and for the WBC in (E) it requires seeing a large portion of the smooth round boundary of the cell.

[VIEW LARGE](#)

[DOWNLOAD SLIDE](#)

## Disclosures

**Gurkan:Dx Now Inc.:** Patents & Royalties; **Xatek Inc.:** Patents & Royalties; **BioChip Labs:** Patents & Royalties; **Hemex Health, Inc.:** Consultancy, Current Employment, Patents & Royalties, Research Funding.

## Author notes

\* Asterisk with author names denotes non-ASH members.

© 2020 by The American Society of Hematology

**Volume 136, Issue Supplement 1**

November 5 2020

[Skip to Main Content](#)

[⟨ Previous Article](#)

[Next Article ⟩](#)

## Potential Articles of Interest

Contribution of Red Blood Cell Derived Extracellular Vesicles to Sickle Red Blood Cell Adhesion Discerned Using an Endothelialized Microfluidic Assay  
Ran An et al., Blood

Thrombin-Induced Endothelial Cell Damage Is Mitigated By Human Anti-Thrombin III in a Microfluidic Device  
William Wulf Lange et al., Blood

Red Blood Cell Adhesion in Adult Patients with Sickle Cell Disease, at Baseline and with Pain, Measured on SCD Biochip Microfluidic Assay  
Boye-Doe et al., Blood

Simultaneous polymerization and adhesion under hypoxia in sickle cell disease  
Dimitrios P. Papageorgiou et al., Proc Natl Acad Sci U S A, 2018

Lung vaso-occlusion in sickle cell disease mediated by arteriolar neutrophil-platelet microemboli  
Margaret F. Bennewitz et al., JCI Insight., 2017

Association Between Endothelial Dysfunction, Biomarkers of Renal Function and Disease Severity in Sickle Cell Disease  
Oluwagbemiga Oluwole Ayoola et al., Kidney360, 2020

---

Powered by **TREND** 

---

[View Metrics](#)

---

---

## Cited By

[Google Scholar](#)

---

 **Email Alerts**

[Article Activity Alert](#)

[Skip to Main Content](#)

[Latest Issue Alert](#)[Current Issue](#)[First edition](#)[All Issues](#)[Collections](#)[Abstracts](#)[Authors](#)[Submit to Blood](#)[About Blood](#)[Subscriptions](#)[Public Access](#)[Permissions](#)[Alerts](#)[Contact Us](#)[Blood Classifieds](#)[Advertising in Blood](#)[Terms and Conditions](#)[Twitter](#)

**American Society of Hematology** / 2021 L Street NW, Suite 900 / Washington, DC 20036 / TEL +1 202-776-0544 /

FAX +1 202-776-0545

[Skip to Main Content](#)

## ASH Publications

---

*Blood*

*Blood Advances*

*Hematology, ASH Education Program*

*ASH Clinical News*

*ASH-SAP*

*The Hematologist*

## American Society of Hematology

---

ASH Home  
Research  
Education  
Advocacy

Meetings  
Publications  
ASH Store

Copyright ©2020 by American Society of Hematology

[Privacy Policy](#)

[Cookie Policy](#)

[Terms of Use](#)

[Contact Us](#)